LA-UR-86-1547

TITLE ANGULAR DEPENDENCE OF MULTILAYER-REFLECTOR DAMAGE THRESHOLDS

LA-UR--86-1547

DE86 011265

AUTHOR(S) BRIAN E. NEWNAM, CHM-6
STEPHEN R. FOLTYN, CHM-5
DENNIS H. GILL, CHM-DO
L. JOHN JOLIN, CHM-5

SUBMITTED TO Laser Induced Damage in Optical Materials: 1984,

Proceedings of the 16th Annual Symposium on Optical Materials for High-Power Lasers, Boulder, CO, Oct. 15-17, 1984.

Angular Dependence of Multilayer-Reflector Damage Thresholds*

Brian E. Newnam, Stephen R. Foltyn, Dennis H. Gill, and L. John Jolin
Los Alamos National Laboratory
Chemistry Division
Los Alamos, New Mexico 87545

The damage resistance of HfO_2/SiO_2 multilayer dielectric reflectors was measured as a function of angle of incidence with 351-nm XeF-laser irradiation. The laser produced nominal 10-ns pulses at a repetition rate of 35 pps. A series of reflectors designed for 0°, 30°, 45°, 60°, 75°, and 85° was tested with an S-plane polarized beam. To account for variations in the separate coating depositions, some of the coating designs were tested at two angles of incidence. At large angles of incidence, we did not observe the anticipated large increases in damage thresholds predicted theoretically on the basis of spatial dilution (1/cosØ) of the intensity at the reflector surface and standing-wave electric fields. For example, the threshold for a reflector designed and tested at 85° was only a factor of 2.5 larger than that of normal-incidence reflectors tested at 0°. Several possible mechanisms to explain this discrepancy were considered.

Key words: Coating defects; free-electron lasers; grazing-incidence reflection; hafnium oxide; laser damage thresholds; multilayer reflectors; multiple-shot laser damage; silicon dioxide; standing-wave electric fields; thin films; ultraviolet reflectors; xenon fluoride lasers.

---

* This work was performed under the auspices of the U. S. Department of Energy.

1. Introduction

Free-electron laser (FEL) oscillators, driven by rf linear accelerators, are being designed for high-average power applications in the ultraviolet to the near infrared from 400 to 1000 nm. The pulse format of these oscillators requires mirrors that will not damage or degrade under high peak intensities and high repetition rates ranging from 10^7 to 10^8 Hz. To function without significant distortion, the resonator mirrors must not be subjected to excessive average-power loading. Thus, very high mirror reflectance is required as well as low optical absorption to minimize the generation of heat and its flow into the water-cooled mirror substrates. Multilayer dielectric (MLD) reflectors are the logical choice for the resonator mirrors since they have demonstrated the highest reflectance values. For example, reflectances greater than 99.99% are now obtained for small-diameter, ion-beam deposited reflectors for 633-nm laser gyro cavities. However, resistance to degradation by the total FEL radiation environment remains to be considered.

It is necessary to include FEL physics in establishing the resonator mirror design. Specifically, high intracavity intensity is required within the magnetic-undulator gain region to obtain efficient conversion of the electron energy to coherent radiation. With undulator lengths ranging from 1 to 10 meters, the optical beam should have both a small waist and low divergence, i.e., a long Rayleigh range. FEL beams have exhibited the desirable characteristic of near-diffraction-limited quality. [1] As a result, very long distances are required between the resonator end mirrors to attain an acceptable intensity loading. However, if the mirror separation becomes too long, the cavity becomes less stable and unavoidable mirror jitter can seriously decrease the overlap of the optical and electron beams and thereby reduce the FEL efficiency

Restriction of the FEL resonator length to minimize the effect of mirror jitter opposes the need for large distances to allow diffraction to dilute the intensity on the mirrors. A solution to this problem is to add a set of slightly curved, intracavity mirrors oriented at large angles, e.g. 85°, to diverge the optical beam to an acceptable intensity level on the end mirrors. Because the FEL radiation is linearly polarized, these intracavity mirrors are oriented for S-polarized reflection only. Theoretically, use at large angles should result in very high damage resistance and less thermal distortion for a given beam intensity.

Since FEL oscillators are a relatively new development, we have given special attention to their mirror needs in the above discussion. However, both excimer laser and FEL oscillator and amplifier optical systems have the common additional requirement for beam-directing mirrors used at non-normal incidence, and mirror damage data is urgently needed to permit realistic design of these external systems.

For metal mirrors, there have been a few measurements of laser damage resistance and optical absorption at large incidence angles. These demonstrated the theoretically predicted $[1/\cos\emptyset]^2$ threshold dependence for S-polarization [2,3]. However, data regarding the angular dependence of MLD reflectors is sparse and has been limited to incidence angles of 0° and 45°.

The present set of experiments was motivated to determine the angular dependence of multiple-shot damage resistance of MLD reflectors for incidence angles from 0° to 85° and S-polarized beams. Conducted at the low repetition rate of 35 pps, these tests did not address the issue of average-power damage thresholds or cw thermal distortion of mirrors which must be evaluated in future test series with lasers operating at high-repetition rates.

Special consideration was given to the possible role of the standing-wave (SW) electric field as a function of angle of incidence because of previous correlations with damage thresholds. From multiple-shot tests using ~10-ns pulses at ultraviolet wavelengths of 248 nm [4], 308 nm [5], and 355 nm [6], we identified the peak SW electric field in the outermost high-index layer as setting the threshold of damage. On this basis, our calculations of the SW fields led us to predict increasingly higher damage thresholds with angle of incidence, but only for S-polarized laser beams. The results of these calculations for the specific reflectors tested in the present experiments are shown in Fig. 1 for incidence angles of 0° and 85° for both S- and P- polarized beams. The cosine intensity-dilution factor is inherently accounted for in the SW field calculations. The SW fields for angles less than 85° are intermediate to the curves shown. If optical damage is correlated with the peak value of $|E/E_i^+|^2$ in the first high-index layer, as would be the case with linear absorption, Fig. 1 indicates that we might expect the damage threshold at 85° to be a factor of 102 X larger than that at normal incidence.

2. Test Specimens

The test specimens were coated by Broomer Labs by electron-beam evaporation with ordinary conditions as used in their commercial production. In addition to the general features listed in Table 1, particular details of the coating depositions included the following: 300 °C substrate temperature, deposition rate of 5 min/QW, 8 X 10^{-5} Torr background pressure with O_2 bleed, and 5 X 10^{-6} Torr initial vacuum. The reflectors were not post baked. For purposes of computing the film thicknesses, Broomer used the refractive indices of 1.51 for SiO_2 and 2.08 for HfO_2, which are typical values at 351 nm.

Because the magnitudes of the SW fields can be strongly affected by film thickness errors, we evaluated the spectral transmittance curves from spectrometer measurements at normal incidence. Comparisons of the design and measured center wavelengths are provided in Table 2. We think that the measured thickness discrepancies should not have influenced the damage thresholds to any great degree.

Table 1. Test samples

Coating materials:	HfO_2 and SiO_2
Design:	$S/(HL)^{11}HL^2/A$ for S-polarization
Deposition process:	Electron gun
Coating vendor:	Broomer Labs
Substrates:	Fused silica (5.1-cm dia.)
	BK-7 glass (6.4 X 12.7 cm)

Table 2. Coating thickness errors

Design Angle	Center Wavelength for Normal Incidence		Deviation[b]
	Design (nm)	Measured (nm)[a]	
0°	351	354	+1%
30°	367	384	+5%
45°	386	403	+4.5%
60°	407	405	-0.5%
75°	426	420	-1.5%
85°	434	425	-2%

[a] Wavelength corresponding to the center frequency midway between 1% transmittance points of the reflection band.

[b] For 0° incidence on a reflector designed for 0°, a 3% thickness error results in ≤1% increase in the SW electric-field peaks. For 85° incidence (S-polarized light) on a reflector designed for 85°, a 10% thickness error results in a 25% increase of the field peak in the uppermost high-index layer and a 20% increase in the uppermost (HW overcoat) low-index layer.

3. Laser Damage Test Conditions

The laser damage test facility depicted in Fig 2 and our standard multiple-shot measurement procedures have been described previously. [4,5] One modification, not shown, was inclusion of multilayer polarizers which we aligned very carefully to obtain a polarization purity of $I_S/I_p \geq 1000$ incident on the samples. In addition, the beam dimensions in the sample plane, which varied with incidence angle, were measured directly with a Reticon silicon-diode linear array. As shown in Table 4, the measured diameters of the near-Gaussian beam did not deviate significantly from the predictions. Naturally, the measured beam sizes were used in calculations of the damage thresholds. Other laser test parameters are listed in the following table.

Table 3. Laser test parameters

Wavelength:	351 nm (XeF)
Polarization:	S-plane with purity $I_S/I_P \geq 1000$
Pulsewidth:	10 ns (FWHM)
Spot-size diameter ($1/e^2$):	0.4 mm, mean value normal to beam
	0.4 mm/cosØ, mean value on sample
Repetition rate:	35 pps
Shots per site:	140 if no damage detected, or ≤140 if damage

Table 4. Angular dependence of the laser beam diameter (vertical plane) at the reflector surface

Angle of Incidence	Predicted Diameter $2w_0/\cos\varnothing$, (mm)	Measured Diameter (mm)	Deviation from $1/\cos\varnothing$
0°	0.128	0.128	---
30°	0.148	0.142	-4%
45°	0.181	0.173	-4%
60°	0.256	0.235	-8%
75°	0.495	0.470	-5%
85°	1.47	---	---

4. Experimental Results

Preliminary to damage tests over the entire range of angles of incidence, the possible threshold variations within a given coating run were determined for the 0° and 30° designs. These threshold values, given in Table 5, indicate a range of ±10 to ±15%. Also, the 4 to 5 J/cm^2 magnitude is about the same as our previous measurements of other reflectors composed of these same coating materials. Since each angle of incidence required a separate coating deposition, we attempted to account for run-to-run variations by testing some of the reflectors at two angles of incidence. We intended to obtain this two-angle registration for each coating design, but only 0° and 30° designs were so evaluated due to decreased coating target area available at the larger angles. For these two designs, the variations were within 10% as shown in Table 6. Predicted differences on the basis of the peak SW electric fields also were small.

The results as a function of the full range of incidence angles are listed in Table 7, and the supporting data from which the threshold values were obtained are presented in the series of Figs. 3. This extensive display of test data is given because of 1) the significance that might be given these results in optical designs of FEL resonators and other beam directing elements, and 2) to allow the reader the opportunity for a thorough examination of these results with the possibility that other interpretations might become evident. We note that the available laser energy was insufficient to reach the saturation fluence (damage at 10 out of 10 test sites) for the 85° case. Figure 4 allows direct comparison of the experimental results for all of the angles of incidence used.

We observed that the damage morphology at high angles of incidence differed from that for near-normal incidence. At the large angles, the damage sites had an elongated triangular pattern, different from the elliptical beam footprint, with the long dimension aligned along the direction of the incident beam.

Table 5. Comparison of damage thresholds of HfO_2/SiO_2 reflectors fabricated in the same coating run

Design- and Test Angle	Sample Identification	Damage Threshold J/cm^2
0°	0-1	4.1
	0-2	4.7
	0-3	5.2
30° (S-polar.)	30-1	4.0
	30-2	4.5

Table 6. Comparison of damage thresholds for HfO_2/SiO_2 reflectors tested at two angles of incidence

Sample Number	Design Angle	Test Angle	Damage Threshold J/cm^2	Peak SW Electric Field[a]
0-1	0°	0°	4.1	0.95
		30°	4.5	0.89
30-1	30°	30°	4.5	0.85
		45°	4.6	0.76

[a] Calculated in the HfO_2 films (for reflectors centered at 351 nm) and normalized to the S-polarized incident field E_o^+.

Table 7. Damage thresholds versus angle of incidence for HfO_2/SiO_2 reflectors tested at the design angle

Design and Test Angle	Damage Threshold J/cm^2	Peak SW Electric Field[a]
0°	4.6 ± 0.5	0.95
30°	4.3 ± 0.4	0.85
45°	5.2	0.72
60°	6.6	0.52
75°	6.9	0.28
85°	11.5 ± 0.5	0.094

[a] Calculated in the HfO_2 films (for reflectors centered at 351 nm) and normalized to the S-polarized incident field E_o^+.

5. Discussion

It is informative to compare the angular dependence of the damage thresholds against the predictions of several possible physical models. One obvious model is that the threshold is determined by the laser fluence incident on the outer surface of the reflector. Because the beam footprint becomes elongated as 1/cosØ, the fluence at the surface is diluted by the 1/cosØ factor. Therefore, in terms of the laser fluence measured normal to the incident beam, which is the value cited when measuring damage thresholds, this model would predict that the threshold should increase as 1/cosØ. The second and third models predict that damage resistance is inversely proportional to some power of the peak SW electric fields in the high-index coating. In one case, the fields were computed for the case of a 100% S-plane polarized incident beam. In the other, the fields were computed as if there were a 100% conversion of the beam to P-polarization.

In Fig. 5, the angular dependence of the measured damage thresholds, normalized to the average result for 0° incidence, is compared to the predictions of the three models considered. Clearly, at large angles the measured damage thresholds fall far below the model predictions for both the 1/cosØ dilution and the S-polarized peak field-squared which assumes linear absorption. For 85° incidence, for example, the damage threshold was only 2.5 times larger than at normal incidence. However, the P-polarized peak-field-squared model underestimated the thresholds. It is worth citing a similar result obtained at the U. K. Rutherford Appleton Laboratories for reflectors designed for S-polarized laser radiation at 248 nm using ThF_4/cryolite films [7]. In that case, the single-shot (15-20 ns pulses) threshold of ~15 J/cm^2 at 86° exceeded that for 0° incidence, ~3 J/cm^2, by only a factor of five.

Unfortunately, we have insufficient data by which to uniquely determine the cause of the unexpectedly low damage thresholds at large angles of incidence. We have, however, speculated on a number of possible mechanisms. We list the most plausible ones for further consideration:

1. Larger surface areas exposed at large angles result in more coating defects being irradiated, thereby increasing the probability of damage.

2. Reflectors designed for large angles of incidence are composed of thicker films which have lower thresholds (more defects).

3. Nonuniform SW electric fields may occur near coating defects, and the near-field diffraction field maxima directly behind opaque coating defects could be very large.

4. Scattered light trapped within the layers by total internal reflection could either increase the effective film absorption or be channeled to absorbing coating defects. See Fig. 6.

5. Pinholes in the coatings could act like light tunnels. At large angles, incident radiation could be funneled into the interior more or less independent of the angle of incidence.

6. The angular dependence of damage may be only a measure of film defects at the air-film interface. Protruding defects could interact with the SW electric-field maxima in air, $2E_0$, which are much larger than those in the interior of the multilayer [8]. With increasing angle, the location of the SW peaks moves away from the air-film interface.

7. The polarization purity of the incident beam ($I_S/I_P \geq 1000$) might have been degraded upon scattering within the multilayers or rotated by coating birefringence. Depolarization of scattered light from multilayers has been observed previously [9]. (Almost total depolarization [$I_S/I_P = 1$] of the entire beam would have been necessary to produce the observed lower thresholds.)

8. The coating depositions for the 60°-, 75°-, and 85°-reflectors may have produced more absorbing films.

Although we have no supporting evidence to absolutely distinguish between the above speculations, we suspect that items 1 to 5 are more plausible than items 6 to 8. Further clarification will require auxiliary tests, e. g., calorimetric measurements of absorption which could detect any unexpected (spatially averaged) increases in reflector absorption at large angles due, for example, to trapped scattered light. If film scatter is responsible for restricted thresholds at large angles, reflectors produced by coating deposition processes that produce films with less scatter should be tested. These processes include rf sputtering, ion-beam sputtering, and ion-assisted electron-beam deposition. According to S. Lu, however, the measured absorption of ion-beam-deposited reflectors for an S-polarized 633 nm beam was the same at 0° and 45° [10].

The experimental data as shown in Figs. 4 and 5 exhibited a second feature that is not understood. For angles of incidence from 0° to 45°, the slopes (% damage/energy fluence) increased as expected, since the spot area was increasing and more defects were irradiated. As first revealed by Foltyn [11], increased irradiation area should result in steeper slopes, but the threshold (0/10 sites damage) should remain essentially the same.

However, for incidence angles from 45° to 85°, the present experimental data produced slopes which declined with increasing angle. There is an opportunity for some clever detective work to explain this.

6. Conclusions

The damage resistance of HfO_2/SiO_2 multilayer dielectric reflectors was measured as a function of angle of incidence from 0° to 85° using S-polarized, 10-ns, 351-nm XeF-laser pulses at 35 pps. At large angles of incidence, we did not observe the anticipated large increases in damage threshold predicted theoretically on the basis of either spatial dilution (1/cosØ) of the intensity at the reflector surface or SW electric fields. For example, the threshold for a reflector designed and tested at 85° was only a factor of 2.5 larger than that of normal-incidence reflectors tested at 0°. The absence of correlation with the peak SW fields is contrary to previous experience with non-quarter-wave reflector designs at UV wavelengths. We have considered several possible mechanisms to explain this discrepancy, but further testing is necessary to prove whether any of these are responsible.

7. References

[1] Newnam, B. E. Capabilities of broadly tunable free-electron lasers. New Lasers for Analytical and Industrial Chemistry. Proc. SPIE 461; 1984. 90-97.

[2] Goldstein, I.; Bua, D.; Horrigan, F. A. Pulsed laser damage to uncoated metallic reflectors. Nat. Bur. Stand. (U. S.) Spec. Publ. 435; 1976. 41-48.

[3] Figueira, J. F.; Thomas, S. J.; Harrison, R. F. Damage thresholds to metal mirrors by short-pulse CO_2 laser radiation. Nat. Bur. Stand. (U. S.) Spec. Publ. 638; 1983. 229-238.

[4] Newnam, B. E.; Foltyn, S. R.; Jolin, L. J.; Carniglia, C. K. Multiple-shot ultraviolet laser damage resistance of nonquarterwave reflector designs for 248 nm. Nat. Bur. Stand. (U. S.) Spec. Publ. 638; 1983. 363-371.

[5] Foltyn, S. R.; Jolin, L. J.; Newnam, B. E. Progress in ultraviolet damage testing at Los Alamos. Nat. Bur. Stand. (U. S.) Spec. Publ. 669; 1984. 266-273.

[6] Carniglia, C. K.; Hart, T. T.; Rainer, F.; Staggs, M. C. Recent damage results on high reflector coatings at 355 nm. Nat. Bur. Stand. (U. S.) Spec. Publ. 688; 1985. 347-353.

[7] M. Lunt, Technical Optics, Ltd., private communication on damage test results of their reflectors as reported to him by F. O'Neill of Rutherford Appleton Laboratory, United Kingdom.

[8] P. A. Temple, Naval Weapons Laboratory, private communication; also, Total internal reflection microscopy: a surface inspection technique. Appl. Opt. 20, 2656 (1981).

[9] J. O. Porteus, Naval Weapons Laboratory, private communication.

[10] S. Lu, Litton Industries, private communication.

[11] Foltyn, S. R. Spotsize effects in laser damage testing. Nat. Bur. Stand. (U.S.) Spec. Publ. 669; 1984. 368-379.

Figure Captions

Figure 1. Standing-wave electric-field distributions in HfO_2/SiO_2 reflectors designed for 0°- and 85°-incidence. Fields are plotted normalized to E_0^+, the incident electric field in air. At large angles such as 85°, the fields for S-polarized radiation are much lower than for normal incidence; modest advantage is attained with P-polarization. For angles smaller than 85°, intermediate field distributions are calculated.

Figure 2. Schematic of the Los Alamos excimer-laser, multiple-shot, laser-damage test facility.

Figures 3a-f. Multiple-shot laser damage test results for 351-nm HfO_2/SiO_2 multilayer reflectors as a function of angle of incidence with S-polarization.

Figure 4. Angle dependence of multiple-shot damage thresholds summarized from test results given in Figs. 3.

Figure 5. Measured damage thresholds normalized to the average result for normal incidence are compared to the predictions of three models: 1) 1/cosØ dilution of the fluence at the reflector surface, 2) inverse of the normalized peak electric-field-squared in the top HfO_2 layer for S-polarized light, and 3) for P-polarization. The measured damage thresholds fall far below the model predictions.

Figure 6. One physical model that may explain the anomalously low damage thresholds at large incidence angles: Scattered light, trapped in the layers by total internal reflection, could either sufficiently raise the effective absorption or channel radiation to absorbing defects.

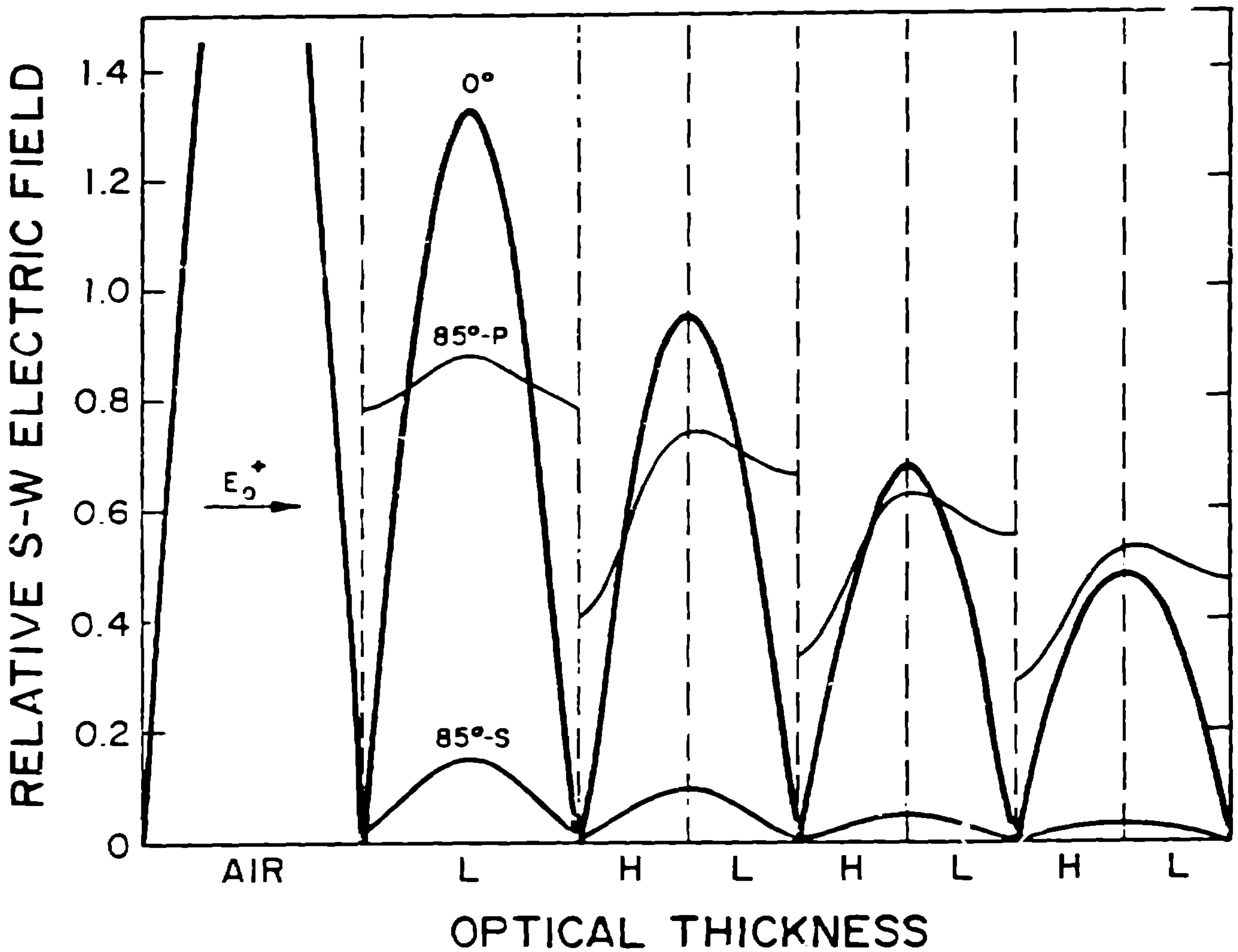
RELATIVE S-W ELECTRIC FIELD
1.4
1.2
1.0
0.8
0.6
0.4
0.2
0
0°
85°-P
85°-S
E_0^+
AIR
L
H
L
H
L
H
L
OPTICAL THICKNESS

CHM-VG-7140

C

MULTIPLE-SHOT LASER DAMAGE TEST FACILITY

- REAL TIME VIDEO MONITORING
- VIDEO RECORDING
- COMPUTER ASSISTED TESTING
- COLOR MICROSCOPY

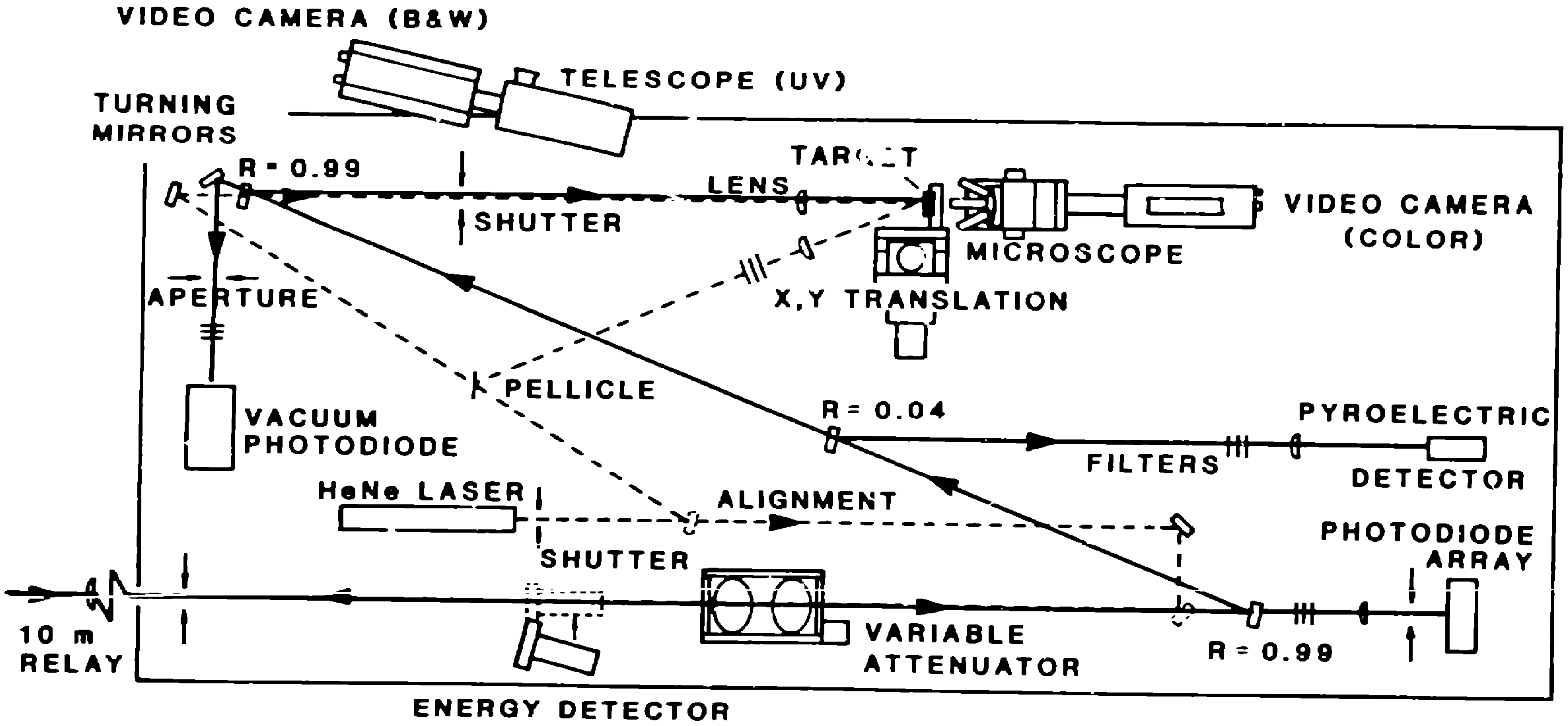

CHM-VG-10,385

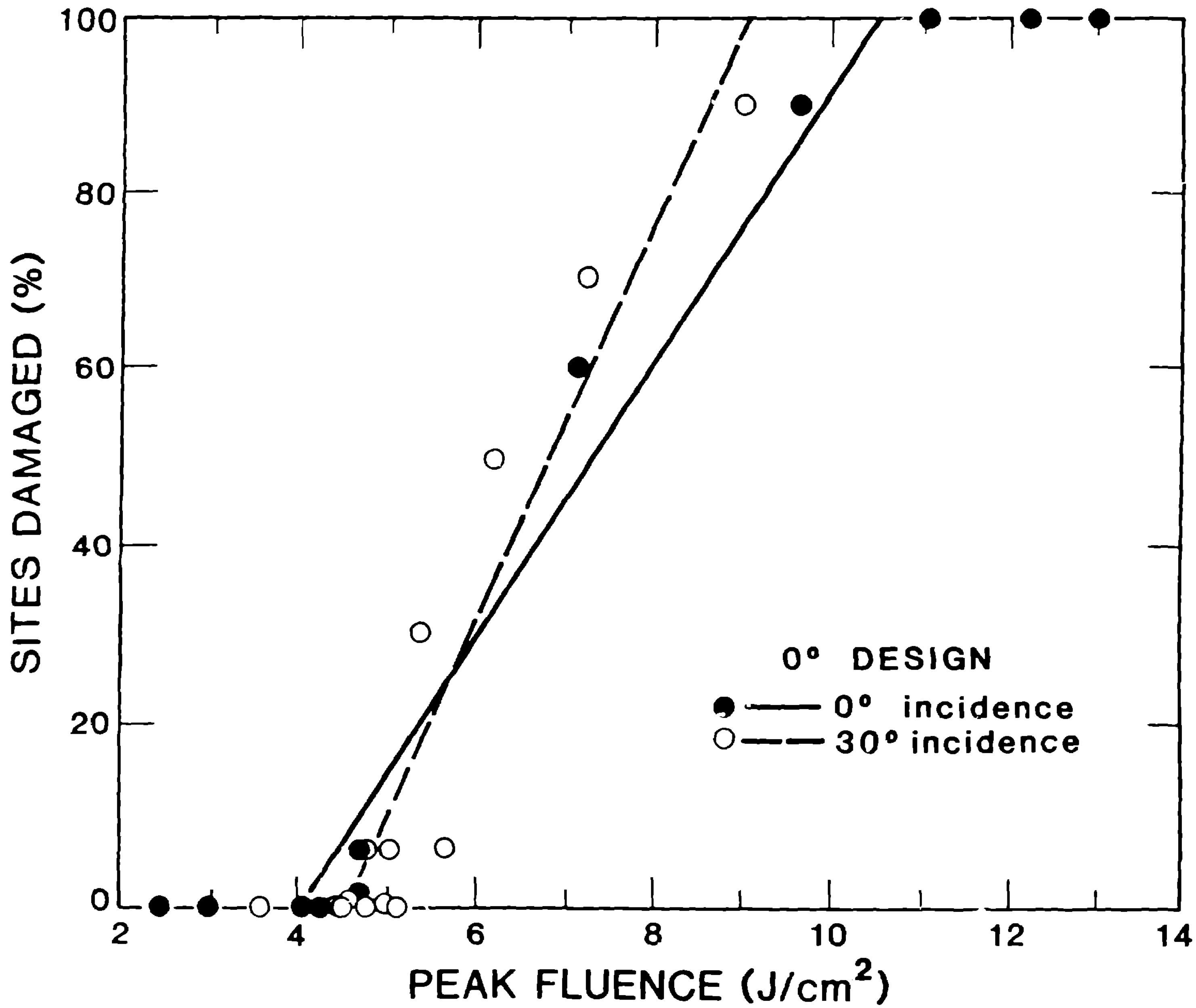

100
80
60
40
20
0
2
4
6
8
10
12
14
SITES DAMAGED (%)
PEAK FLUENCE (J/cm²)
0° DESIGN
0° incidence
30° incidence

CHM-VG-10,502

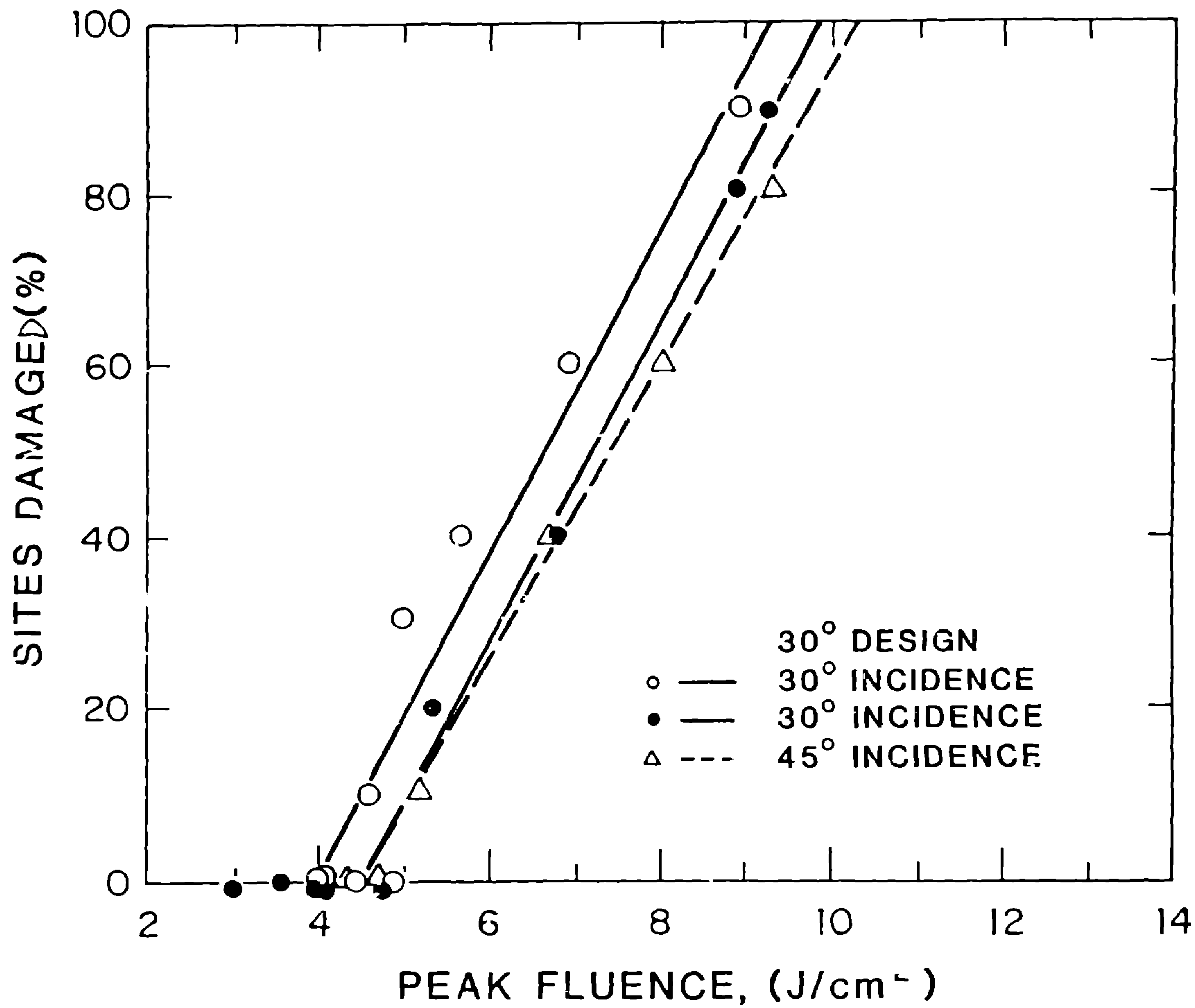

SITES DAMAGED (%)
100
80
60
40
20
0
2
4
6
8
10
12
14
PEAK FLUENCE, (J/cm²)
30° DESIGN
30° INCIDENCE
30° INCIDENCE
45° INCIDENCE

CHM-VG-10,514

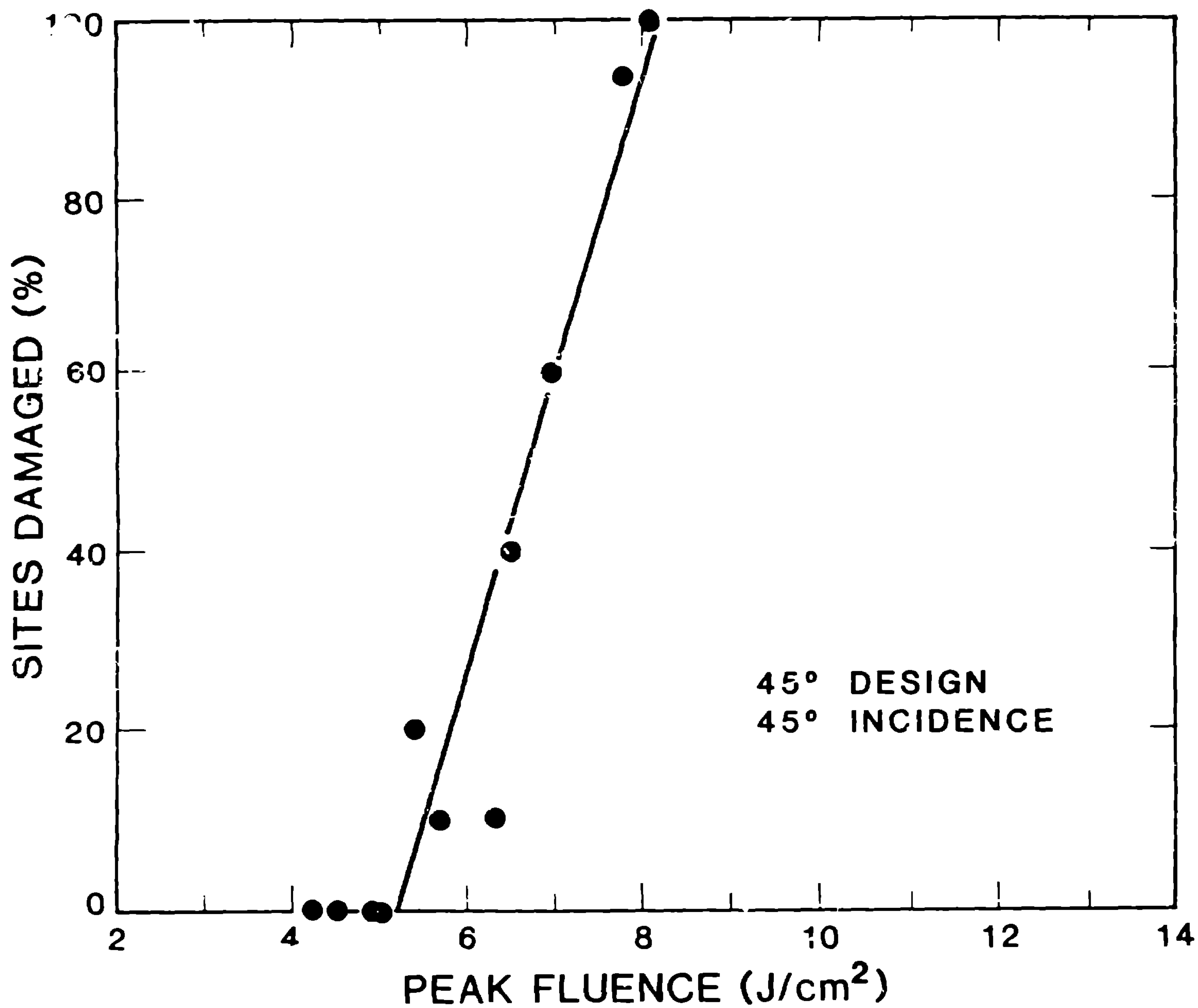

SITES DAMAGED (%)
0
20
40
60
80
2
4
6
8
10
12
14
PEAK FLUENCE (J/cm²)
45° DESIGN
45° INCIDENCE

CHM-VG-10,497

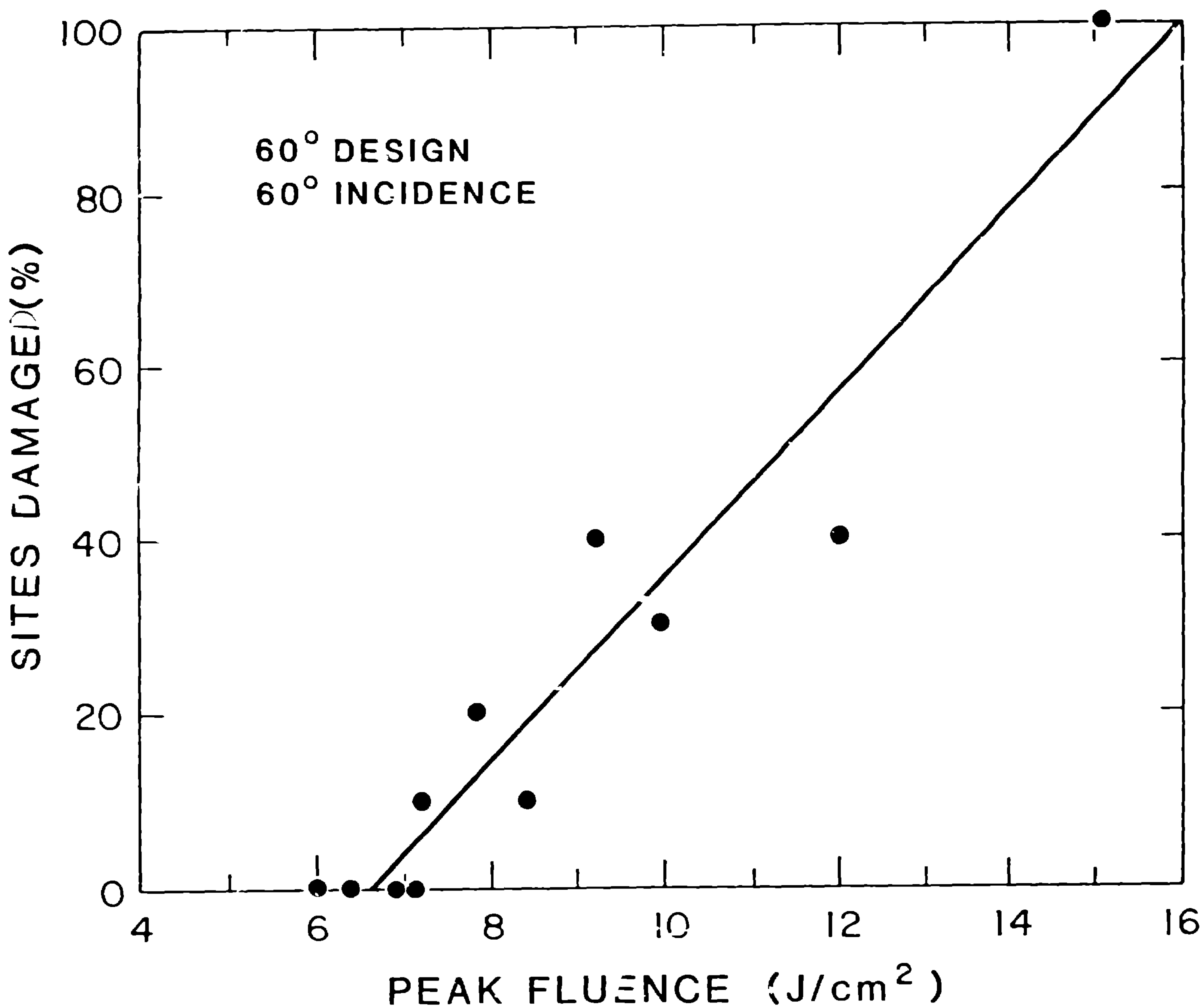

60° DESIGN
60° INCIDENCE
SITES DAMAGED (%)
0
20
40
60
80
100
4
6
8
10
12
14
16
PEAK FLUENCE (J/cm²)

CHM-VG-10,513

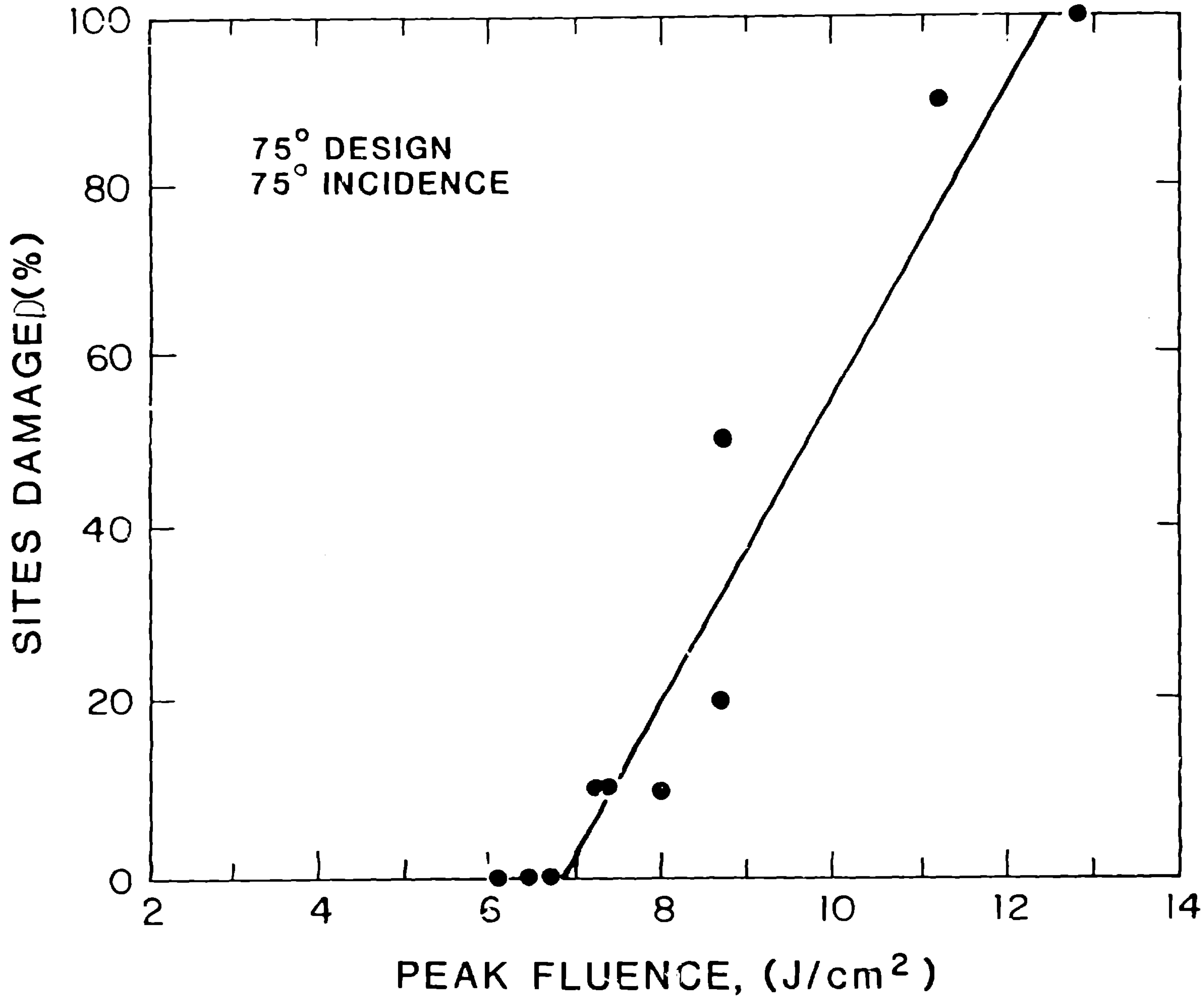
75° DESIGN
75° INCIDENCE
SITES DAMAGED (%)
PEAK FLUENCE, (J/cm²)
0
20
40
60
80
100
2
4
6
8
10
12
14

CHM-VG-10,515

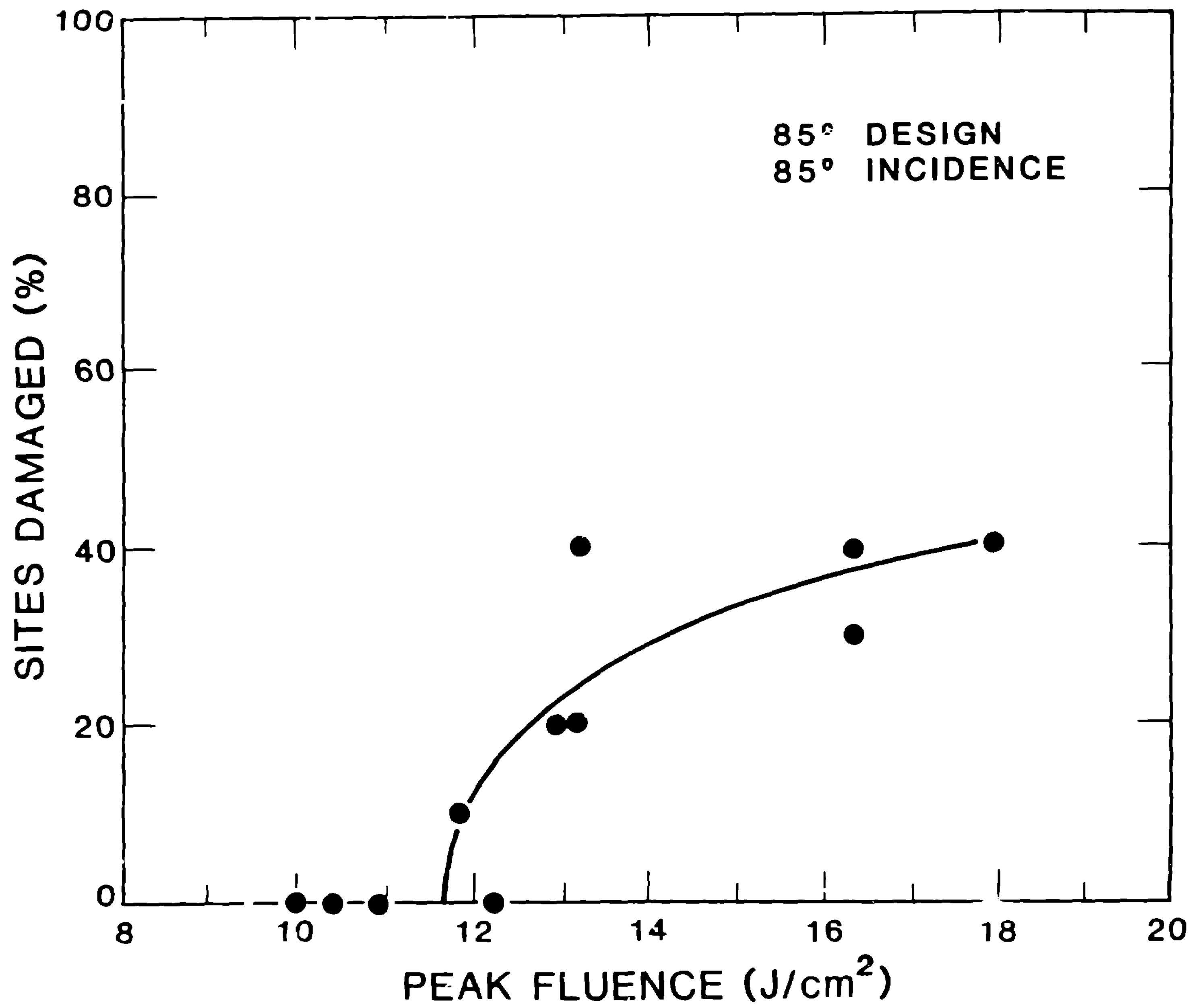

85° DESIGN
85° INCIDENCE
SITES DAMAGED (%)
100
80
60
40
20
0
8
10
12
14
16
18
20
PEAK FLUENCE (J/cm²)

CHM-VG-10,498

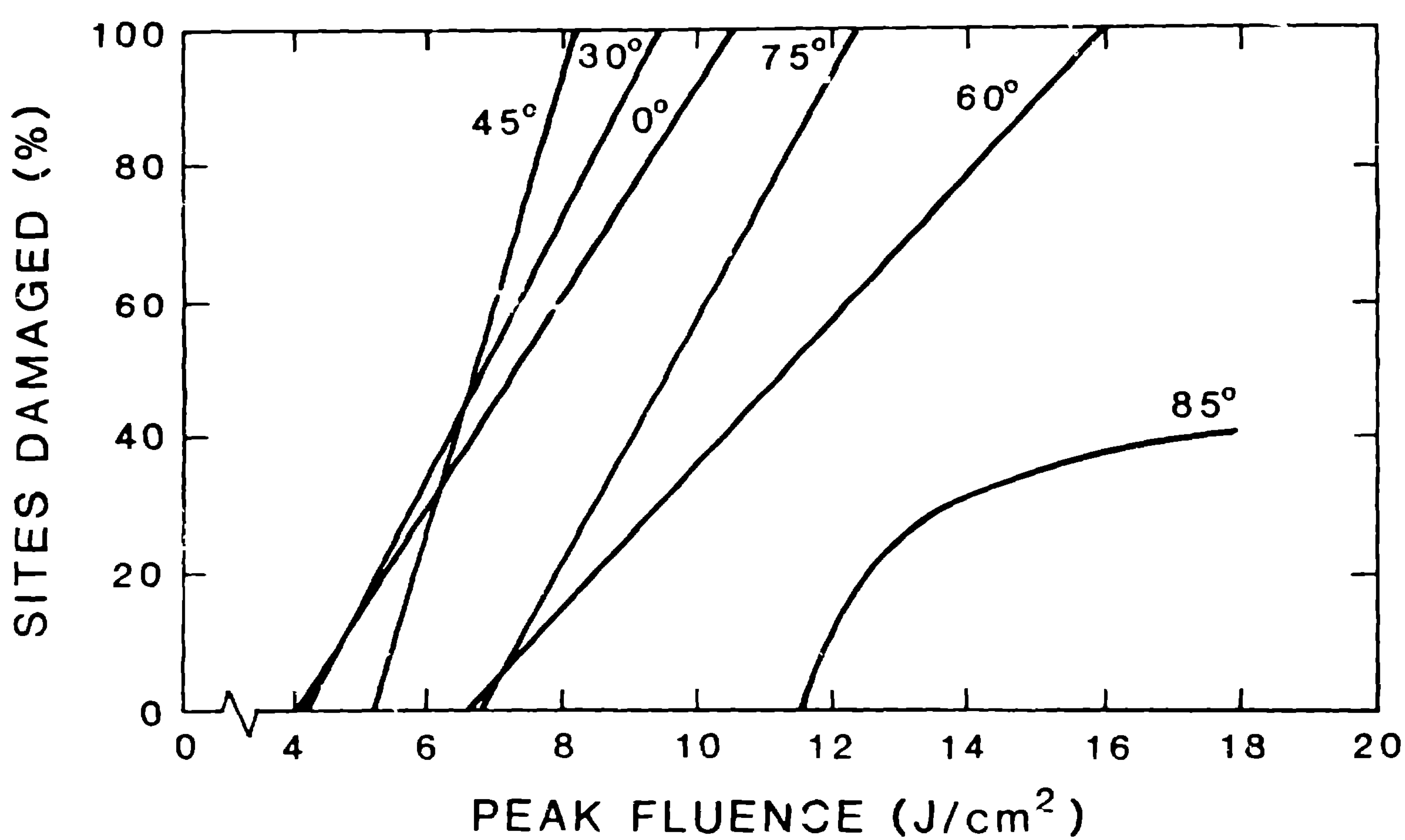

CHM-VG-10,494

Fig. 4

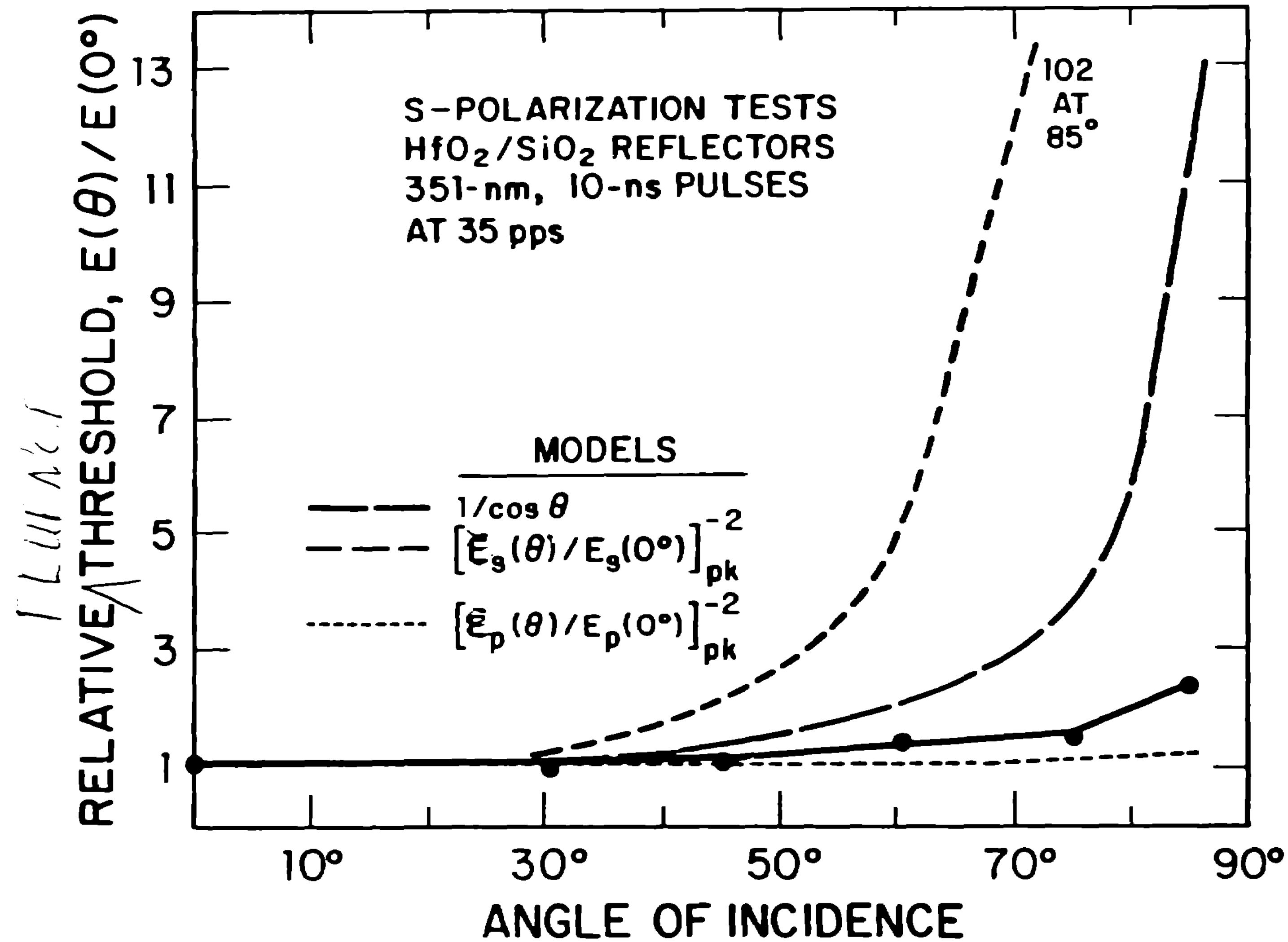
S-POLARIZATION TESTS
HfO2/SiO2 REFLECTORS
351-nm, 10-ns PULSES
AT 35 pps
102 AT 85°
MODELS
1/cos θ
[Es(θ)/Es(0°)]pk -2
[Ep(θ)/Ep(0°)]pk -2
RELATIVE THRESHOLD, E(θ)/E(0°)
ANGLE OF INCIDENCE
1
3
5
7
9
11
13
10°
30°
50°
70°
90°

CHM-VG-6978

TRAPPED SCATTERED LIGHT INCREASES ABSORPTION

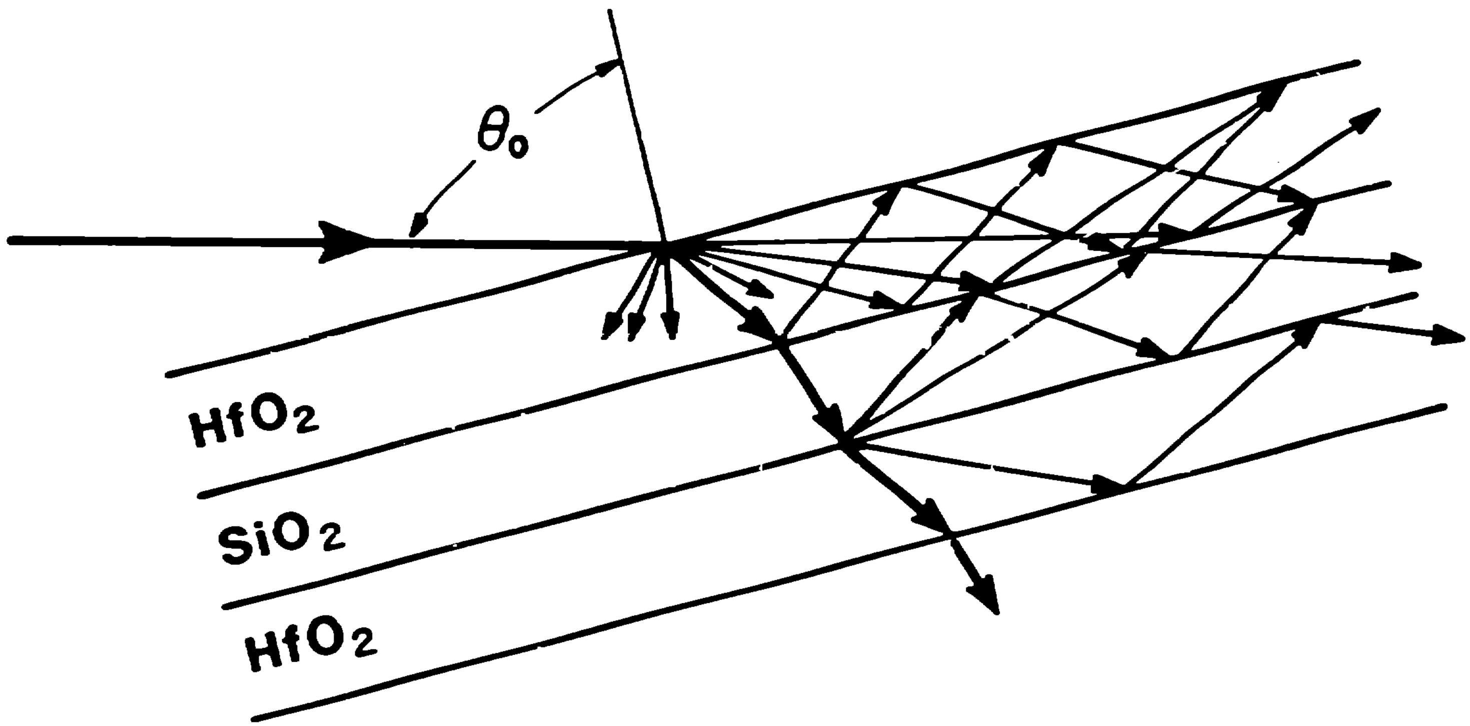

CHM-VG-8525